Electrochromic nickel oxide films and their compatibility with potassium hydroxide and lithium perchlorate in propylene carbonate: Optical, electrochemical and stress-related properties

Rui-Tao Wen*, Gunnar A. Niklasson and Claes G. Granqvist

Department of Engineering Sciences, The Ångström Laboratory, Uppsala University,

P. O. Box 534, SE-75121 Uppsala, Sweden

Abstract

Porous nickel oxide films were deposited onto unheated indium tin oxide coated glass substrates by reactive dc magnetron sputtering. These films had a cubic NiO structure. Electrochromic properties were evaluated in 1 M potassium hydroxide (KOH) and in 1 M lithium perchlorate in propylene carbonate (Li–PC). Large optical modulation was obtained for ~500-nm-thick films both in KOH and in Li–PC (~70 % and ~50 % at 550 nm, respectively). In KOH, tensile and compressive stress, due to expansion and contraction of the lattice, were found for films in their bleached and colored state, respectively. In Li–PC, compressive stress was seen both in colored and bleached films. Durability tests with voltage sweeps between –0.5 to 0.65 V vs Ag/AgCl in KOH showed good durability for 10,000 cycles, whereas voltage sweeps between 2.0 to 4.7 V vs Li/Li^+ in Li–PC yielded significant degradation after 1000 cycles.

Keywords: nickel oxide, thin film, electrochromism, stress, transmittance, durability

*Corresponding author: Ruitao.Wen@angstrom.uu.se

1. Introduction

The atmospheric content of carbon dioxide has risen from ~315 ppm in the late 1950s to ~400 ppm in 2013, and the increase rate has tripled—from ~0.7 to ~2.1 ppm per year—during the same period. The increased amount of CO_2 is largely an effect of fossil fuel burning and other human activities and is generally believed to have far reaching consequences with regard to human life, as recently reported by the Intergovernmental Panel on Climatic Change, under the auspices of the United Nations [1]. Drastic reductions in the use of fossil fuel, as well as a global transition to renewable energy sources, are needed to combat the effects of the growing CO_2 concentration. The buildings sector is of particular interest in this context since it accounts for 30 to 40 % of today's use of primary energy globally [2]. This fraction tends to increase and, to take a specific example, the buildings' share of the primary energy consumption in the USA was 41 % in 2010, whereas it was only 34 % in 1980 [3].

Energy savings in buildings is a huge and largely untapped resource for CO_2 abatement [4]. Many "green" technologies—often with nanostructural attributes—can be implemented in buildings [5–7], and energy efficient fenestration is a particularly attractive option that can offer also improved indoor comfort [8] and financial benefits [9]. Windows are usually weak links in the buildings' energy systems and typically let in or out too much energy that needs to be compensated by cooling or heating. It is obvious that "smart windows", with variable throughput of solar energy and visible light, can diminish the energy expenditure. Electrochromic (EC) "smart windows" have been under development for decades and are currently being implemented in buildings [10]. These windows normally include a multilayer structure with two different EC thin oxide films joined by an electrolyte, and this three-layer stack is surrounded by transparent electrical conductors [11]. Optical absorption is modulated when a voltage is applied between the electrodes and is associated with charge transfer between the EC films [11].

Electrochromism in tungsten oxide films has been known for about forty years; these films color under charge insertion (cathodically) [12]. In practical constructions, the W oxide films need to be complemented by films that ideally color under charge extraction (anodically). Iridium oxide films have this desired property, and devices based of W-oxide-based and Ir-oxide-based thin films have been cycled electrochemically for millions of times [11]. However Ir oxide is too expensive for large scale applications, even when diluted with

less costly Ta oxide [13,14] or Sn oxide [15–17], and nickel-oxide-based alternatives have been studied since the mid-1980s [18–20]. Devices incorporating W-oxide-based and Ni-oxide-based films have attracted much interest [21], and EC "smart windows" using this combination of materials are currently introduced on the market [10]. However, the Ni-oxide-based films are still in need of refinement, and research on Ni-oxide-based films is pursued vigorously; recent (2009 and later) studies have been published on such films prepared by evaporation [22], sputtering [23–27], chemical vapor deposition [28], various wet-chemical techniques such as sol–gel deposition [29–36] and chemical bath deposition [37–44], and electrodeposition [44–49]. Electrochromic Ni-oxide-based films have been made also by electrophoretic deposition of Ni hydroxide nanoparticles [50] and from Ni oxide pigments deposited from water dispersion [51]. The electrochromism of binary Ni-based mixed oxides have attracted much attention during recent years, and results have been presented for such oxides containing Li [52–54], C [55,56], N [57], F [58], Al [59], Ti [60], V [61,62], Mn [49], Co [33], Cu [63], and W [25]. Ternary Ni-based oxides or nanocomposites containing Li–Al [64], Li–Zr [65], and Li–W [66] have given particularly interesting results. Finally we note that work has been reported also for number of hybrid materials of NiO–Q, where Q stands for poly(3,4-ethylenedioxythiophene) [67], polypyrrole [68], polyaniline [42], graphene oxide [69], and LiPON [70].

Generally speaking, the EC and other properties of Ni-oxide-based films can be improved by adding a second element, which explains the intense interest in them as noted above. The present paper lays a foundation for a comprehensive investigation of electrochromism in the Ni–Ir oxide system—with a scope that is similar to the one in our recent work on the electrochromism in the full Ni–W system [23,25,71–73]—but is of interest also in its own right. Data on pure Ir oxide immersed in propionic acid, potassium hydroxide (KOH), and lithium perchlorate in propylene carbonate (Li–PC) were presented recently [74]. Below we investigate pure Ni oxide in KOH and Li–PC under experimental conditions that were carefully chosen in order to allow direct comparison with data on Ir oxide (propionic acid was not considered since Ni oxide is not stable in acids).

2. Experimental details

2.1 Thin film deposition

Thin films of nickel oxide were made by reactive dc magnetron sputtering in a coating system based on a Balzers UTT 400 unit. The substrates were 5 × 5 cm^2 glass plates with transparent and electrically conducting layers of In_2O_3:Sn (known as ITO) having a sheet resistance of 60 Ω. No substrate heating was used. The target was a 5-cm-diameter plate of metallic nickel (99.95 %), and the target–substrate separation was 13 cm. Pre-sputtering took place in argon (99.998 %) for 5 minutes, and oxygen (99.998 %) was then introduced. During deposition, the O_2/Ar gas-flow ratio was set at a constant value of 2.5 %. The total pressure during sputtering was maintained at ~4 Pa, and the power at the target was 200 W. Film uniformity was ensured by substrate rotation during the depositions. The film thickness *d* was determined by surface profilometry using a DektakXT instrument. Most films had a thickness *d* of ~500 nm. Further experimental details are given elsewhere [75].

2.2 Structural and compositional characterization

Film structures were determined by X-ray diffraction (XRD) using a Siemens D5000 diffractometer operating with CuK_α radiation at a wavelength λ_x = 0.154 nm. The measurement took place at room temperature with a grazing incidence angle of one degree in parallel beam geometry with a 2θ (θ was defined as the diffraction angle) between 10° and 90°. The step size was 0.0200°. Structure and phase composition were obtained by comparison with the Joint Committee on Powder Diffraction Standards (JCDPS) data base.

Linear grain sizes *D* were determined by use of Scherrer's formula [76], i.e.,

$$D = \frac{k\lambda_x}{\beta \cos\theta} \quad , \tag{1}$$

where $k \sim 0.9$ is a dimensionless "shape factor", β is the full width at half-maximum of an X-ray diffraction peak, and θ denotes diffraction angle.

Morphology and porosity of the films were characterized by scanning electron microscopy (SEM) using a LEO 1550 FEG Gemini instrument with an acceleration voltage of 10 to 15 kV.

Elemental compositions and atomic concentrations were determined by Rutherford Backscattering Spectrometry (RBS) at the Uppsala Tandem Laboratory, specifically using 2MeV ^{4}He ions back scattered at an angle of 170 degrees. The RBS data were fitted to a model of the film–substrate system by use of the SIMNRA program [77].

Film density ρ was computed from

$$\rho = \frac{MN_s}{n_a N_A d} \quad , \tag{2}$$

where M is molar mass, N_s is areal density of atoms, n_a is the number of atoms in a molecule, and N_A is Avogadro's constant.

2.3 Electrochemical and optical measurements

Cyclic voltammetry (CV) was performed in a three-electrode electrochemical cell by use of a computer-controlled ECO Chemie Autolab/GPES Interface. The Ni oxide film served as working electrode and was electrochemically cycled in electrolytes consisting of 1 M KOH and 1 M Li–PC. For the KOH electrolyte, the counter electrode was a Pt foil and the reference electrode was Ag/AgCl; the voltage range was –0.5 to 0.65 V vs Ag/AgCl. In the case of Li–PC, both counter and reference electrodes were Li foils, and the voltage range was 2.0 to 4.7 V vs Li/Li^+ which, importantly, was chosen to be the same as in our earlier investigation of Ir oxide films [74]. The voltage sweep rate was 10 mV/s, except for studies of long-term cycling durability when it was 50 mV/s.

Optical transmittance measurements were recorded in situ during electrochemical cycling of Ni-oxide-based films in the 380–800 nm wavelength range by using a fiber-optical instrument from Ocean Optics. The electrochemical cell was positioned between a tungsten halogen lamp and the detector, and the 100-%-level was taken as the transmittance recorded before immersion of the sample in the electrolyte.

Electrochemical and optical measurements were employed to record the coloration efficiency (CE), which is defined as the difference in optical density per amount of charge exchange (ΔQ). Specific data were obtained from

$$CE = \frac{\log\left(\frac{T_{bl}}{T_{col}}\right)}{\Delta Q} \quad , \tag{3}$$

where T_{bl} and T_{col} are the transmittance values for films in their fully bleached and colored states, respectively, and it is assumed that the related modulation in reflectance is small. It is desirable for most electrochromic devices, including "smart windows", that the CE should be as large as possible.

3. Results and discussion

Fig. 1 shows SEM images of a typical ~500-nm-thick as-deposited Ni oxide film. Panels (a) and (b) show that the film has a distinct surface morphology with triangular features having linear extents of ~40 nm or less. The cross-sectional image in Fig. 1(c) indicates a columnar nanostructure. This structure is as expected from the thin film deposition conditions—with a high pressure in the sputter plasma and a low substrate temperature—and is consistent with zone 1 in a "Thornton diagram" [78]. The columnar features are favorable for electrochromism [79].

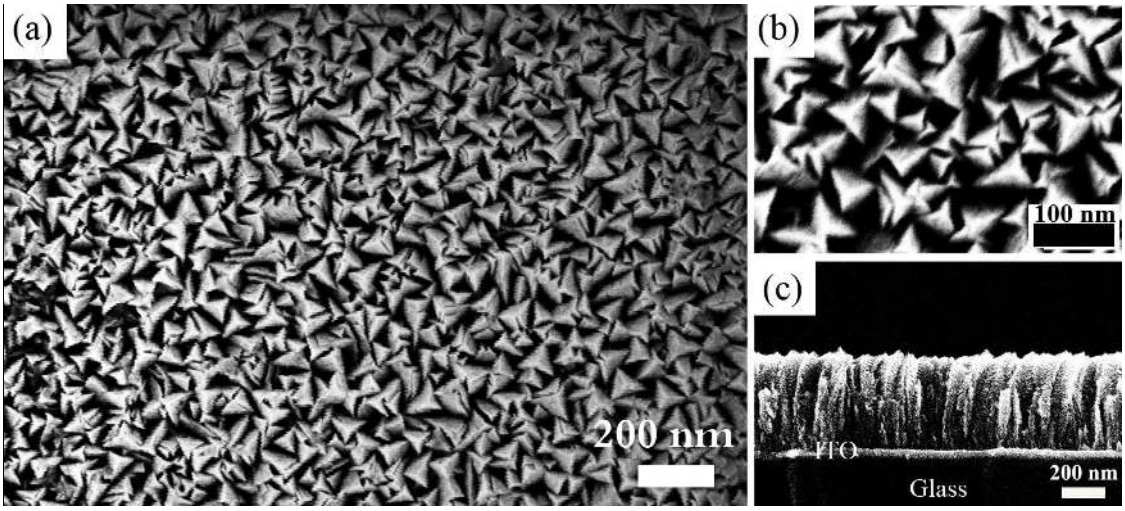

Fig. 1. SEM images of a Ni oxide thin film. Panels (a) and (b) are top views at different magnifications, and panel (c) shows a cross-sectional view of the film on an ITO-coated glass substrate.

RBS data showed that as-deposited films could be represented as $NiO_{1.22}$. It should be noted that the hydrogen content cannot be determined by RBS. The film density was 3.9 g/cm^3, which is consistent with earlier results [23,80].

3.1 Nickel oxide films in KOH: Electrochemical, optical and structural properties

Electrochemical cycling of Ni oxide in alkaline media has been investigated for decades, initially in the context of electrical batteries and later also for electrochromics [11]. Several different electrochemical reaction schemes have been proposed, and it appears that the

reactions can proceed via the exchange of H^+ and OH^- depending on the nature of the film as well as on the electrolyte. Further complications arise since the films can evolve during electrochemical cycling [20,44]. A detailed study on sputter-deposited Ni-oxide-based films in 1 M KOH was presented by Avendaño et al. [80,81] and pointed at the general applicability of the Bode reaction scheme, which is well established for batteries [82,83]; specifically the bleached and colored states were associated with $Ni(OH)_2$ and NiOOH, respectively, and the EC reaction can be written, schematically, as

$$Ni(OH)_2 \leftrightarrow NiOOH + H^+ + e^- \quad (4)$$

or, alternatively,

$$Ni(OH)_2 + OH^- \leftrightarrow NiOOH + H_2O + e^- \ , \quad (5)$$

where e^- denotes electrons.

Fig. 2 displays cyclic voltammograms of Ni-oxide-based films in the KOH electrolyte for the first 15 cycles. Broad oxidation and reduction features appear, and it is evident that some minor evolution takes place during the initial cycles, but that the properties are stable after a few cycles. The charge density during the voltammetric cycling shows some unbalance during the first cycle but then remains at 15.6 ± 0.4 mC/cm^2 for cycles 2 to 15, as apparent from Fig. 3.

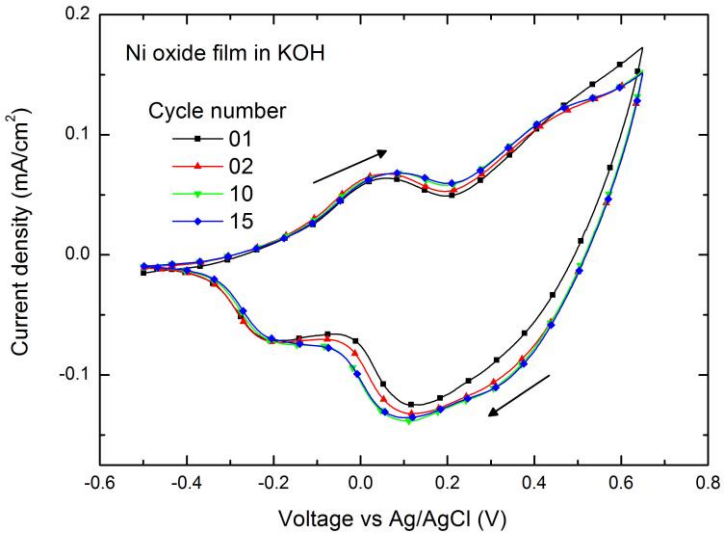

Fig. 2. Cyclic voltammograms for a ~500-nm-thick Ni oxide film in 1 M KOH; the voltage sweep rate was 10 mV/s and arrows indicate sweep direction.

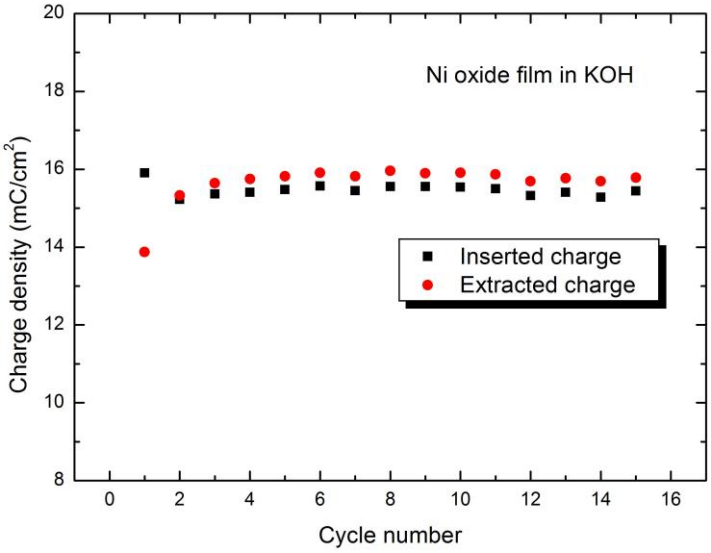

Fig. 3. Charge density corresponding to the endpoints of cyclic voltammograms such as those in Fig. 2. The charge inserted/extracted was taken to be positive.

Fig. 4(a) reports spectral transmittance for Ni-oxide-based films in as-deposited state and after full coloration and bleaching. Inserted photos show the bleached and colored states. The optical modulation at a mid-luminous wavelength of 550 nm is as large as ~70 %, as apparent in Fig. 4(b). The fact that the transmittance is lower after 15 CV cycles than for the first cycle can be reconciled with the increased charge extraction seen in Fig. 3. The coloration efficiency was evaluated from Eq. 3 and was found to be 44 ± 2 cm^2/C at 550 nm, which is of the expected magnitude [11,23,80].

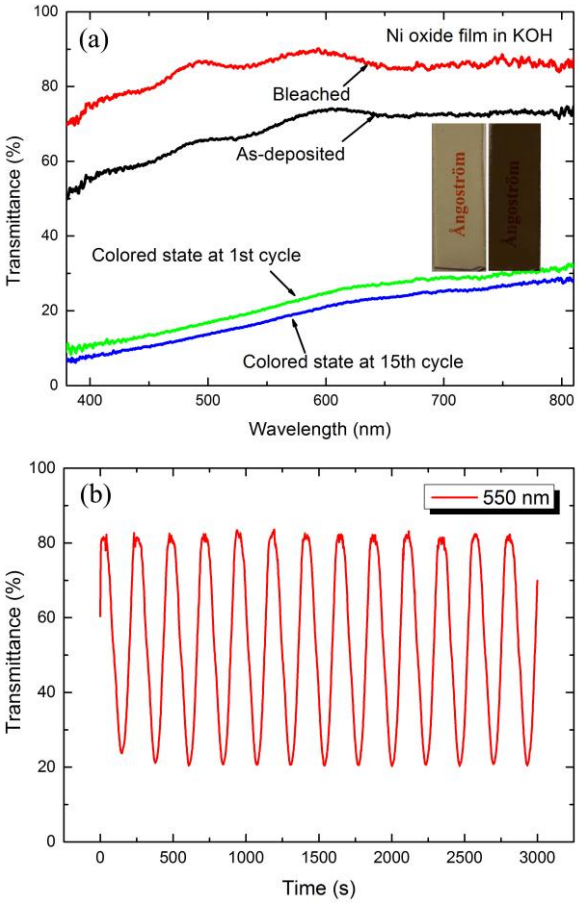

Fig. 4. Panel (a) shows spectral transmittance of a ~500-nm-thick Ni oxide film in 1 M KOH; data were taken on films in as-deposited, colored and bleached states. Inserted images refer to Ni oxide in fully bleached and colored states. Panel (b) reports corresponding optical transmittance modulation at a wavelength of 550 nm.

XRD patterns of Ni-oxide-based films in as-deposited, bleached and colored states are reported in Fig. 5. The latter data were taken after 15 CV cycles. The XRD peaks can be assigned to NiO with a cubic structure (JCDPS card number 47–1049), and additional peaks originate from ITO. No diffraction features could be associated with $Ni(OH)_2$ or NiOOH, and it appears that the XRD signal emerges from crystalline Ni oxide grains on which thin and/or heavily disordered hydrogen-containing phases have formed. The grain size was estimated to be ~40 nm, as obtained from the broadening of the diffraction peaks denoted (111), (200), (220), and (311) (cf. Eq. 1). This grain size is consistent with our SEM images and is somewhat larger than in earlier work [23,80].

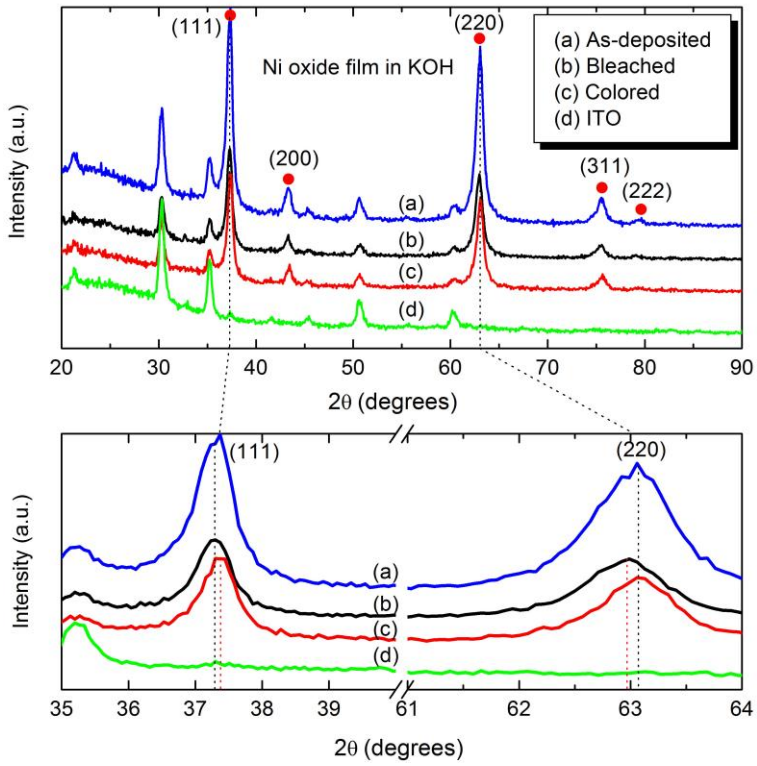

Fig. 5. X-ray diffractograms of a ~500-nm-thick Ni oxide film, backed by ITO, in 1 M KOH. Data (in arbitrary units, a.u.) were taken on films in as-deposited, colored and bleached states as well as for the ITO-coated substrate. The diffraction peaks indicated by red dots are assigned to the shown lattice planes in cubic NiO. Upper panel shows survey scans and lower panel shows magnifications of the (111) and (220) peaks and illustrate displaced peak positions (indicated by dotted vertical lines).

A detailed analysis of the XRD data for films in as-deposited, colored and bleached states indicated that the peak positions were different for colored and bleached Ni-oxide-based films. Specifically, the most prominent diffraction peaks—corresponding to the (111) and (220) lattice planes—occurred at somewhat smaller angles for bleached films than for colored films. Thus the transition from coloration to bleaching is associated with lattice expansion and ensuing evolution from compressive to tensile stress [84].

3.2 Nickel oxide films in Li–PC: Electrochemical, optical and structural properties

Nickel oxide can show electrochromism in Li-containing electrolytes. As discussed by Passerini et al. [85–88], the Li intercalation proceeds via a two-step process with an initial "activation" by

$$NiO + yLi^+ + ye^- \rightarrow Li_yNiO \quad (6)$$

followed by a reversible reaction capable of going reversibly between bleached Li_yNiO and colored $Li_{(y-x)}NiO$ according to

$$Li_yNiO \leftrightarrow Li_{(y-z)}NiO + zLi^+ + ze^- \quad . \quad (7)$$

Figs. 6 to 9 below show the electrochemical, optical and structural properties of Ni-oxide-based films in 1 M Li–PC in a way that allows easy comparison with analogous data for such films in 1 M KOH as given in Figs. 2 to 5. Cyclic voltammograms are shown in Fig. 6. The shape of the curves deviates from the corresponding data in Fig. 2, which indicates that the electrochemistry for the charge insertion and extraction is different in Li–PC and KOH, and, more importantly, the voltammograms evolve during the 15 initial scans in the voltage range from 2.0 to 4.7 V vs Li/Li^+. This evolution can be seen more clearly in data on charge density upon CV cycling, and Fig. 7 shows that the charge density drops distinctly during the first few charge insertions, which can be understood as an effect of "activation" of the Ni-oxide-based film according to reaction (6) above. Subsequent amounts of charge insertion and extraction differ by a constant value of ~1.4 mC/cm^2 after the fourth CV cycle, and these amounts decline monotonically upon extended voltammetric cycling, which points at irreversible electrochemical reactions leading to continuous sample degradation. We note that no similar effect was found for CV cycling in the 2.0 – 4.7 V vs Li/Li^+ range for our earlier study of Ir-oxide-based films [74].

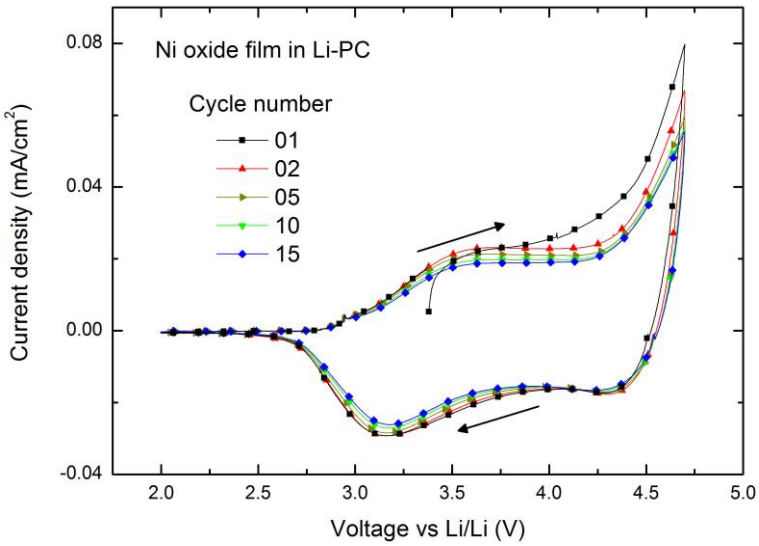

Fig. 6. Cyclic voltammograms for a ~500-nm-thick Ni oxide film in 1 M Li–PC; the voltage sweep rate was 10 mV/s and arrows indicate sweep direction.

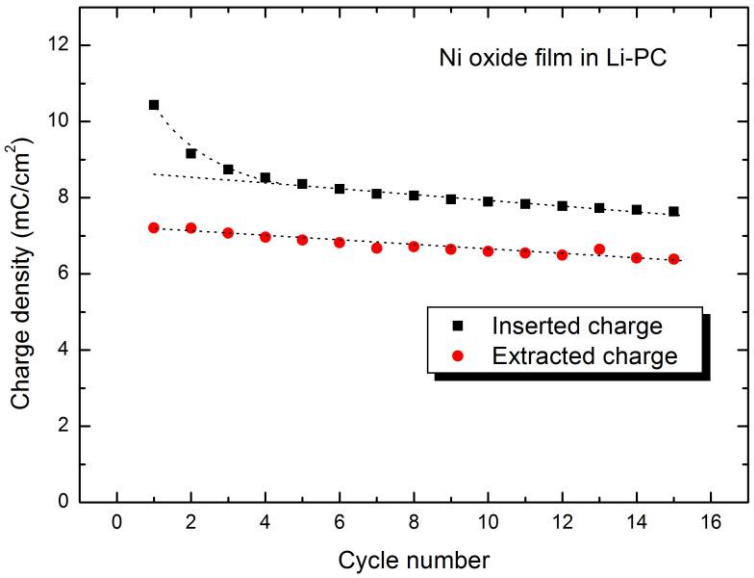

Fig. 7. Charge density corresponding to the endpoints of cyclic voltammograms such as those in Fig. 6. Data points are joined by dotted lines for convenience. The charge inserted/extracted was taken to be positive.

Fig. 8(a) illustrates spectral transmittance data for Ni-oxide-based films in as-deposited states and after 15 CV cycles in Li–PC. Inserted photos show the bleached and colored states. The overall shapes of the curves are similar to those in Fig. 4 for films in KOH, and the mid-luminous transmittance modulation is ~50 %, as indicated by Fig. 8(b). The CE was found to be ~44 cm^2/C, i.e., the same as for films in KOH.

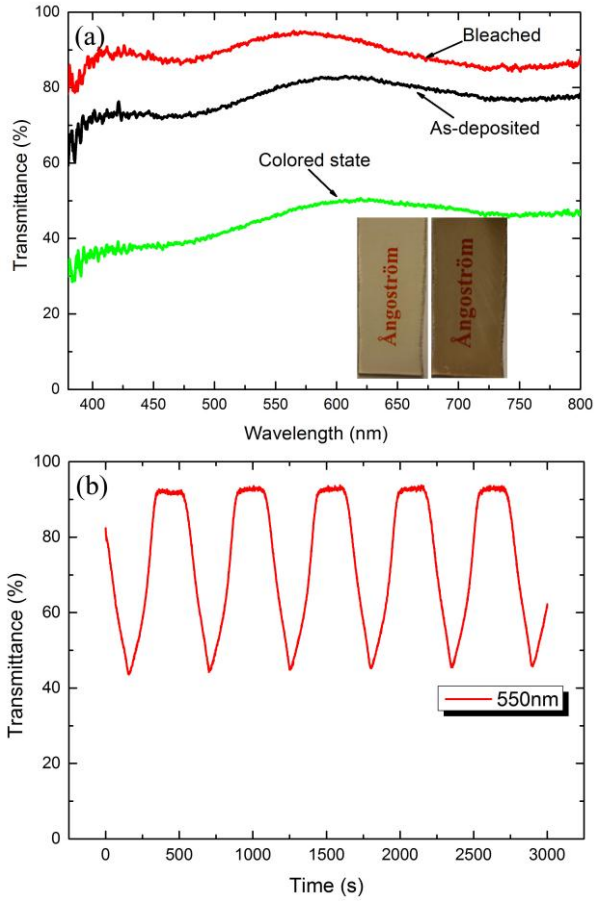

Fig. 8. Panel (a) shows spectral transmittance of a ~500-nm-thick Ni oxide film in 1 M Li–PC; data were taken on films in as-deposited state and after 15 coloration and bleaching cycles. Inserted images refer to Ni oxide in fully bleached and colored states. Panel (b) reports corresponding optical transmittance modulation at a wavelength of 550 nm.

XRD data are given in Fig. 9. Survey scans in panel (a) for as-deposited films and for films that had undergone 15 coloration–bleaching cycles in Li–PC look very similar to analogous data for films in KOH as shown in Fig. 5. The details differ, however, and the main diffraction peaks corresponding to the (111) and (220) lattice planes are shifted slightly towards higher diffraction angles for colored as well as bleached films, which implies a shrinkage of the separation between these lattice planes compared to their separation in as-deposited films. This effect is connected with the irreversible Li insertion and has been noted also in earlier work on lithiated Ni oxide [52–54,89]. It is associated with compressive stress whose origin is not known.

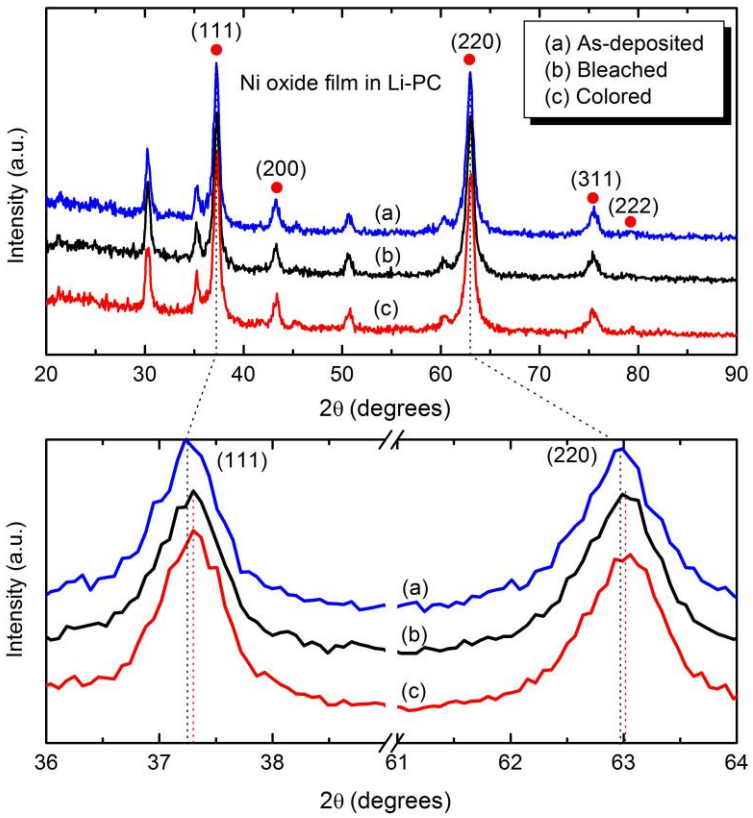

Fig. 9. X-ray diffractograms of a ~500-nm-thick Ni oxide film in 1 M Li–PC. Data (in arbitrary units, a.u.) were taken on films in as-deposited, colored and bleached states. The diffraction peaks indicated by red dots are assigned to the shown lattice planes in cubic NiO. Unassigned peaks are due to ITO, as shown in Fig. 5. Upper panel shows survey scans and lower panel shows magnifications of the (111) and (220) peaks and illustrate displaced peak positions (indicated by the vertical dotted lines).

3.3 Durability assessment of nickel oxide films in KOH and Li–PC

Cycling durability is important for most applications of electrochromism and is essential for EC "smart windows". Voltammetric cycling was performed as described above although at a higher voltage sweep rate of 50 mV/s.

Fig. 10(a) shows data taken in 1 M KOH. Degradation progresses slowly and the charge capacity was 9.5 mC/cm^2 and 7.2 mC/cm^2 after 1,000 and 10,000 cycles, whereas it was 9.9 mC/cm^2 after the second cycle. Significant degradation was observed after 15,000 cycles and was due to structural disintegration of the film at the electrolyte–air interface. Degradation was much faster in 1 M Li–PC, as shown in Fig. 10(b). Now only 67 % and 46 % of the initial charge capacity remained after 100 and 1000 cycles, and no electrochemical activity was noted after 2000 cycles.

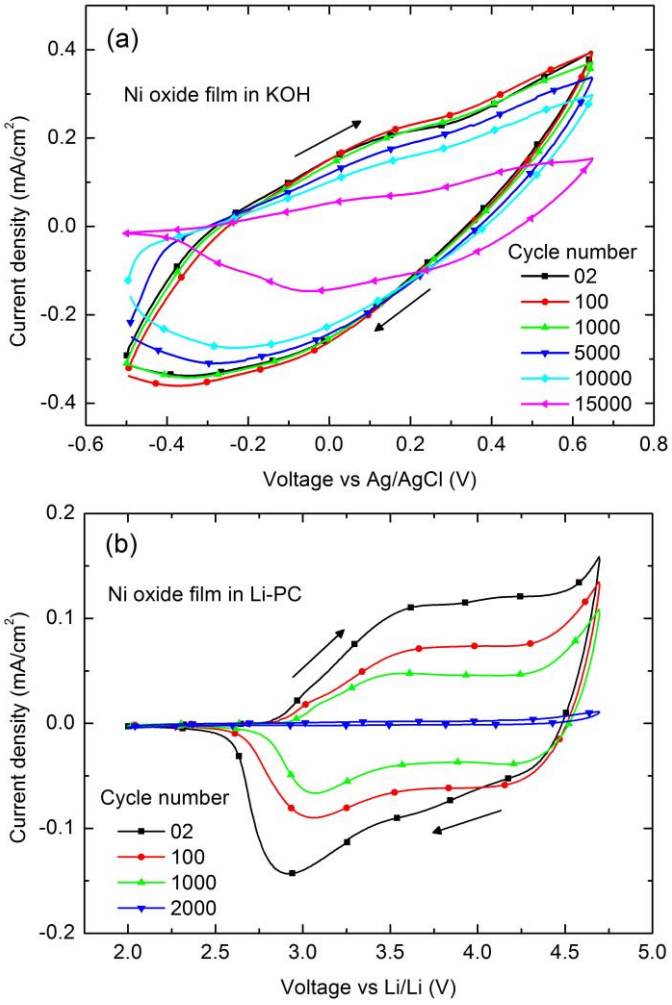

Fig. 10. Cyclic voltammograms of ~500-nm-thick Ni oxide film in 1 M KOH (panel a) and 1 M Li–PC (panel b); the voltage sweep rate was 50 mV/s and arrows indicate sweep direction.

4. Conclusions

Ni oxide films with a thickness of ~500 nm were prepared by reactive dc magnetron sputtering onto ITO-coated glass. The films had a columnar nanostructure and a density that was lower than that of bulk NiO. X-ray diffraction showed that the films had a cubic NiO structure. Cyclic voltammetry and in situ optical transmittance measurements were performed on films that were cycled between –0.5 and 0.65 V vs Ag/AgCl in 1 M KOH and between 2.0 and 4.7 V vs Li/Li$^+$ in 1 M Li–PC. Pronounced electrochromism was found, and the mid-luminous transmittance modulation was 70 % in KOH and ~50 % in Li–PC. X-ray diffraction data showed that tensile stress was present during bleaching in KOH whereas compressive stress occurred during coloring. Compressive stress was found for both bleached and colored

films in Li–PC. The stresses may contribute to the cycling durability of electrochromic Ni-oxide-based films. Extended color–bleach cycling of the films showed good durability for 10,000 cycles in KOH, whereas films degraded strongly already after 1000 cycles in Li–PC.

The voltage sweep ranges were chosen to enable direct comparisons with data for Ir oxide films in earlier work of ours [74]. These Ir oxide films were very stable for electrochemical cycling in the voltage interval where the Ni-oxide-based films were decomposed. Hence our results in the present work serve as a baseline for in-depth studies of Ni–Ir-oxide-based electrochromic films and of devices based on those.

Acknowledgments

We are thankful to Andreas Mattsson for assistance with magnetron sputtering and to Shu-Yi Li for SEM measurements. This work was financially supported by the European Research Council under the European Community's Seventh Framework Program (FP7/2007–2013)/ERC Grant Agreement No. 267234 (GRINDOOR). Additional support was received from the Swedish Research Council.

References

[1] IPCC, 2013: Climate Change 2013: The Physical Basis. Contribution of Working Group I to the Fifth Assessment Report of the Intergovernmental Panel on Climate Change, edited by L. Alexander et al.; www.climatechange2013.org/images/uploads/WGIAR5_WGI-12Doc2b_FinalDraft_All.pdf

[2] UNEP, Buildings and Climate Change: Status, Challenges and Opportunities, United Nations Environment Programme, Paris, France, 2007.

[3] 2010 Buildings Energy Data Book, U.S. Department of Energy, Washington, USA, 2011; http://buildingsdatabook.eere.energy.gov/.

[4] B. Richter, D. Goldston, G. Crabtree, L. Glicksman, D. Goldstein, D. Greene, D. Kammen, M. Levine, M. Lubell, M. Savitz, D. Sperling, F. Schlachter, J. Scofield, J. Dawson, How America can look within to achieve energy security and reduce global warming, Rev. Modern Phys. 80 (2008) S1-S109.

[5] G.B. Smith, C.G. Granqvist, Green Nanotechnology: Solutions for Sustainability and Energy in the Built Environment, CRC Press, Boca Raton, FL, USA, 2010.

[6] F. Pacheco-Torgal, M.V. Diamanti, A. Nazari, C.G. Granqvist, editors, Nanotechnology in Eco-Efficient Construction, Woodhead, Cambridge, UK, 2013.

[7] F. Pacheco Torgal, M. Mistretta, A. Kaklauskas, C.G. Granqvist, L.F. Cabeza, editors, Nearly Zero Energy Building Refurbishment, Springer, Berlin Heidelberg, Germany, 2013.

[8] R.D. Clear, V. Inkarojrit, E.S. Lee, Subject responses to electrochromic windows, Energy Buildings 38 (2006) 758-779.

[9] P. Eichholtz, N. Kok, J.M. Quigley, Doing Well by Doing Good? Green Office Buildings, Am. Econ. Rev. 100 (2010) 2492-2509.

[10] C.G. Granqvist, Oxide electrochromics: An introduction to devices and materials, Sol. Energy Mater. Sol. Cells 99 (2012) 1-13.

[11] C.G. Granqvist, Handbook of Inorganic Electrochromic Materials, Elsevier, Amsterdam, The Netherlands, 1995.

[12] S.K. Deb, Optical and photoelectric properties and colour centres in thin films of tungsten oxide, Philos. Mag. 27 (1973) 801-822.

[13] J. Backholm, A. Azens, G.A. Niklasson, Electrochemical and optical properties of sputter deposited Ir–Ta and Ir oxide thin films, Sol. Energy Mater. Sol. Cells 90 (2006) 414-421.

[14] J. Backholm, G.A. Niklasson, Optical properties of electrochromic iridium oxide and iridium–tantalum oxide thin films in different colouration states, Sol. Energy Mater. Sol. Cells 92 (2008) 1388-1392.

[15] T. Niwa, O. Takai, All-solid-state reflectance-type electrochromic devices using iridium tin oxide film as counter electrode, Thin Solid Films 518 (2010) 5340-5344.

[16] T. Niwa, O. Takai, Low-Temperature Crystallization of Silicon Films Directly Deposited on Glass Substrates Covered with Yttria-Stabilized Zirconia Layers, Jpn. J. Appl. Phys. 49 (2010) 105801-11.

[17] S.U. Yun, S.J. Yoo, J.W. Lim, S.H. Park, I.Y. Cha, Y.-E. Sung, Enhanced Electrochromic Properties of Ir–Ta Oxide Grown Using a Cosputtering System Sensors and Displays: Principles, Materials, and Processing, J. Electrochem. Soc. 157 (2010) J256-J260.

[18] J.S.E.M. Svensson, C.G. Granqvist, Electrochromic hydrated nickel oxide coatings for energy efficient windows: Optical properties and coloration mechanism, Appl. Phys. Lett. 49 (1986) 1566-1568.

[19] J.S.E.M. Svensson, C.G. Granqvist, Electrochromism of nickel-based sputtered coatings, Sol. Energy Mater. 16 (1987) 19-26.

[20] W. Estrada, A.M. Andersson, C.G. Granqvist, Electrochromic nickel ‐ oxide ‐ based coatings made by reactive dc magnetron sputtering: Preparation and optical properties, J. Appl. Phys. 64 (1988) 3678-3683.

[21] G.A. Niklasson, C.G. Granqvist, Electrochromics for smart windows: thin films of tungsten oxide and nickel oxide, and devices based on these, J. Mater. Chem. 17 (2007) 127-156.

[22] B. Subramanian, M.M. Ibrahim, K.R. Murali, V.S. Vidhya, C. Sanjeeviraja, M. Jayachandran, Structural, optoelectronic and electrochemical properties of nickel oxide films, J. Mater. Sci: Mater. Electron. 20 (2009) 953-957

[23] S. Green, J. Backholm, P. Georén, C.G. Granqvist, G.A. Niklasson, Electrochromism in nickel oxide and tungsten oxide thin films: Ion intercalation from different electrolytes, Sol. Energy Mater. Sol. Cells 93 (2009) 2050–2055.

[24] S.V. Green, M. Watanabe, N. Oka, G.A. Niklasson, C.G. Granqvist, Y. Shigesato, Electrochromic properties of nickel oxide based thin films sputter deposited in the presence of water vapor, Thin Solid Films 520 (2012) 3839–3842.

[25] S.V. Green, C.G. Granqvist, G.A. Niklasson, Structure and optical properties of electrochromic tungsten-containing nickel oxide films, Sol. Energy Mater. Sol. Cells 126 (2014) 248-259.

[26] H. Ueta, Y. Abe, K. Kato, M. Kawamura, K. Sasaki, H. Itoh, Ni oxyhydroxide thin films prepared by reactive sputtering using O_2 + H_2O mixed gas, Jpn. J. Appl. Phys. 48 (2009) 015501-015504.

[27] Y. Abe, T. Suzuki, M. Kawamura, K. Sasaki, H. Itoh, Electrochromic properties of NiOOH thin films prepared by reactive sputtering in an H_2O atmosphere in various aqueous electrolytes, Sol. Energy Mater. Sol. Cells 99 (2012) 38-42.

[28] R.A. Patil, R.S. Devan, J.-H. Lin, Y.-R. Ma, P.S. Patil, Y. Liou, Efficient electrochromic properties of high-density and largr-area arrays of one-dimensional NiO nanorods, Sol. Energy Mater. Sol. Cells 112 (2013) 91-96.

[29] K.K. Purushothaman, M. Dhanashankar, G. Muralidharan, Preparation and characterization of F doped SnO_2 films and electrochromic properties of FTO/NiO films, Current Appl. Phys. 9 (2009) 67-72.

[30] K.K. Purushothaman, G. Muralidharan, The effect of annealing temperature on the electrochromic properties of nanostructured NiO films, Sol. Energy Mater. Sol. Cells 93 (2009) 1195-1201.

[31] K.K. Purushothaman, G. Muralidharan, Nonporous NiO based electrochromic window, Funct. Mater. Lett. (2009) 143-145.

[32] K.K. Purushothaman, G. Muralidharan, Enhanced electrochromic performance of nanoporous NiO films, Mater. Sci. Semicond. Process. 14 (2011) 78-83.

[33] K.K. Purushothaman, G. Muralidharan, Electrochromic properties of nickel oxide and mixed Co/Ni oxide films prepared via sol–gel route, J. Non-Cryst. Solids 358 (2012) 354-359.

[34] A. Sawaby, M.S. Selim, S.Y. Marzouk, M.A. Mostafa, A. Hosny, Structure, optical and electrochromic properties of NiO thin films, Physica B 405 (2010) 3412-3420.

[35] S.H. Park, J.W. Lim, S.J. Yoo, I.Y. Cha, Y.-E. Sung, The improving electrochromic performance of nickel oxide film using aqueous N,N-dimethylaminoethanol solution, Sol. Energy Mater. Solar Cells 99 (2012) 31-37.

[36] D.S. Dalavi, R.S. Devan, R.S. Patil, Y.-R. Ma, P.S. Patil, Electrochromic performance of sol–gel deposited NiO thin films, Mater. Lett. 90 (2013) 60-63.

[37] H. Huang, S.X. Lu, W.K Zhang, Y.P. Gan, C.T. Wang, L. Yu, X.Y. Tao, Photoelectrochromic properties of NiO film deposited on an N-doped TiO_2 photocatalytical layer, J. Phys. Chemistry Solids 70 (2009) 745-749.

[38] M.-K. Lee, C.-H. Fan, Electrochromic characterization of nickel oxide films grown on ITO/glass by liquid phase deposition, J. Electrochem. Soc. 156 (2009) D395-D399.

[39] H. Huang, L. Jiang, W.K. Zhang, Y.P. Gan, X.Y. Tao, H.F. Chen, Photoelectrochromic properties and energy storage of $TiO_{2-x}N_x$/NiO bilayer thin films, Sol. Energy Mater. Sol. Cells 94 (2010) 355-359.

[40] H. Huang, J. Tian, W.K. Zhang, Y.P. Gan, X.Y. Tao, X.H. Xia, J.P. Tu, Electrochromic properties of porous NiOthin film as a counter electrode for NiO/WO_3 complementary electrochromic window, Electrochim. Acta 56 (2011) 4281-4286.

[41] A.I. Inamdar, A.C. Sonavane, S.M. Pawar, Y.S. Kim, J.H. Kim, P.S. Patil, W. Jung, H. Im, D.-Y. Kim, H. Kim, Electrochromic and electrochemical properties of amorphous nickel hydroxide films, Appl. Surf. Sci. 257 (2011) 9606-9611.

[42] F. Švegl, A. Šurca Vuk, M. Hajzeri, L. Slemenik Perše, B. Orel, Electrochromic properties of $Ni_{(1-x)}O$ and composite $Ni_{(1-x)}O$-polyaniline films prepared by the peroxo soft chemistry route, Sol. Energy Mater. Sol. Cells 99 (2012) 14-25.

[43] D.S. Dalavi, R.S. Devan, R.S. Patil, Y.-R. Ma, M.-G Kang, J.-H. Kim, P.S. Patil, Electrochromic properties of dandelion flower like nickel oxide thin films, J. Mater. Chem. C 1 (2013) 1035-1039.

[44] Y. Ren, W.K. Chim, L. Guo, H. Tanoto, J. Pan, S.Y. Chiam, The coloration and degradation mechanisms of electrochromic nickel oxide , Sol. Energy Mater. Sol. Cells 116 (2013) 83-88.

[45] F. Liu, X. Zhang, K.-W. Zhu, Y. Song, Z.-H. Shi, B.-X. Feng, Facile fabrication of NiO_xH_y films and their unique electrochromic properties, J. Mater. Sci. 44 (2009) 6028-6034.

[46] A.C. Sonavane, A.I. Inamdar, P.S. Shinde, H.P. Deshmukh, R.S. Patil, P.S. Patil, Efficient electrochromic oxide thin films by electrodeposition, J. Alloys Cpds. 489 (2010) 667-673.

[47] Y.F. Yuan, X.H. Xia, J.B. Wu, Y.B. Chen, J.L. Yang, S.Y. Guo, Enhanced electrochromic properties of ordered porous nickel oxide thin film prepared by self-assembled colloidal crystal template-assisted electrodeposition, Electrochiim. Acta 56 (2011) 1208-1212.

[48] C.-C. Liao, Lithium-driven electrochromic properties of electrodeposited nickel oxide hydroxide electrodes, Sol. Energy Mater. Sol. Cells 99 (2012) 26-30.

[49] T. Yoshino, K. Kobayashi, S. Araki, K. Nakamura, N. Kobayashi, Electrochromic properties of electrochemically fabricated nanostructure nickel oxide and manganese oxide films, Sol. Energy Mater. Sol. Cells 99 (2012) 43-49.

[50] M. Vidotti, S.I. Córdoba de Torresi, Electrostatic layer-by-layer and electrophoretic depositions as methods for electrochromic nanoparticle immobilization, Electrochim. Acta 54 (2009) 2800-2804.

[51] M. Mihelčič, I. Jerman, F. Švegl, A. Šurca Vuk, L. Slemenik Perše, J. Kovač, B. Orel, U. Posset, Electrochromic $Ni_{1-x}O$ pigment coatings and plastic film-based $Ni_{1-x}O/TiO_2$ device with transmissive light modulation, Sol. Energy Mater. Sol. Cells 107 (2012) 175-187.

[52] T. Kubo, Y. Nishikitani, Y. Sawai, H. Iwanaga, Y. Sato, Y. Shigesato, Electrochromic properties of Li_xNi_yO films deposited by RF magnetron sputtering, J. Electrochem. Soc. 156 (2009) H629-H633.

[53] R.C. Tenent, D.T. Gillaspie, A. Miedaner, P.A. Parilla, C.J. Curtis, A.C. Dillon, Fast-switching electrochromic Li^+-doped NiO films by ultrasonic spray deposition, J. Electrochem. Soc. 157 (2010) H318-H322.

[54] H. Moulki, D.H. Park, B.-K. Min, H. Kwon, S.-J. Hwang, J.-H. Choy, T. Toupance, G. Campet, A. Rougier, Improved electrochromic performances of NiO based thin films by lithium addition: From single layers to devices, Electrochim. Acta 74 (2012) 46-52.

[55] Y.-S. Lin, D.-J. Lin, P.-J. Sung, S.-W. Tien, Atmospheric-pressure plasma-enhanced chemical vapour deposition of electrochromic organonickel oxide thin films with an atmospheric pressure plasma jet, Thin Solid Films 532 (2013) 36-43.

[56] Y.-S. Lin, D.-J. Lin, L.-Y. Chiu, S.-W. Lin, Lithium electrochromism of atmospheric pressure plasma jet-synthesized NiOxCy thin films, J. Solid State Electrochem. 16 (2012) 2581-2590.

[57] F. Lin, D.T. Gillaspie, A.C. Dillon, R.M. Richards, C. Engtrakul, Nitrogen-doped nickel oxide thin films for enhanced electrochromic applications, Thin Solid Films 527 (2013) 26-30.

[58] N.K. Shrestha, M. Yang, P. Schmuki, Self-ordered nanoporous nickel oxide/fluoride composite film with strong electrochromic contrast, Electrochem. Solid State Lett. 13 (2010) C21-C24.

[59] D. Mondal, G. Villemure, Effect of the presence of $[Co(bpy)3]^{2+}$ on the electrochromic responses of films of a redox active Ni–Al-layered double hydroxide, J. Electroanal. Chem. 628 (2009) 67-72.

[60] K. Zhang, X.Q. Zhang, C.X. Chang, S.J. Zhang, X.C. Wang, D.L. Sun, M.A. Aegerter, Electrochromic behavior of NiO–TiO2 films prepared with dodecyl sulfonate added to the sol, Sol. Energy Mater. Solar Cells 114 (2013) 192-198.

[61] Y.-S. Lin, P.-W. Chen, D.-J. Lin, Electrochromic performance of NiV_xO_y thin films deposited onto flexible PET/ITO substrates by reactive plasma sputtering for flexible electrochromic devices, Thin Solid Films 518 (2010) 7416-7420.

[62] J.-M. Ye, Y.-P. Lin, Y.-T. Yang, J.-T. Chang, J.-L. He, Electrochromic properties of $Ni(V)O_x$ films deposited via reactive magnetron sputtering with a 8V–92Ni alloy target, Thin Solid Films 519 (2010) 1578-1582.

[63] L. Zhao, G. Su, W. Liu, L. Cao, J. Wang, Z. Dong, M. Song, Optical and electrochemical properties of Cu-doped NiO films prepared by electrochemical deposition, Appl. Surf. Sci. 257 (2011) 3974-3979.

[64] F. Lin, D. Nordlund, T.-C. Weng, R.G. Moore, D.T. Gillaspie, A.C. Dillon, R.M. Richards, C. Engtrakul, Hole doping in Al-containing nickel oxide materials to improve electrochromic performance, ACS Appl. Mater. Interfaces 5 (2013) 301-309.

[65] F. Lin, D. Nordlund, T.-C. Weng, D. Sokaras, K.M. Jones, R.B. Reed, D.T. Gillaspie, D.G.J. Weir, R.G. Moore, A.C. Dillon, R.M. Richards, C. Engtrakul, Origin of electrochromism in high-performing nanocomposite nickel oxide, ACS Appl. Mater. Interfaces 5 (2013) 3643-3649.

[66] D. Gillaspie, A. Norman, C.E. Tracy, J.R. Pitts, S.-H. Lee, A. Dillon, Nanocomposite counter electrode materials for electrochromic windows, J. Electrochem. Soc. 157 (2010) H328-H331.

[67] X.-H. Xia, J.-P. Tu, J. Zhang, X.H. Huang, X.-L. Wang, W.K. Zhang, H. Huang, Multicolor and fast electrochromism of nanoporous NiO/poly(3,4-ethylenedioxythiophene) composite thin films, Electrochem. Commun. 11 (2009) 702-705.

[68] A.C. Sonnavane, A.I. Inamdar, D.S. Dalavi, H.P. Deshmukh, P.S. Patil, Simple and rapid synthesis of NiO/PPy thin films with improved electrochromic performance, Electrochim. Acta 55 (2010) 2344-2351.

[69] G.-F. Cai, J.-P. Tu, J. Zhang, Y.-J. Mai, Y. Lu, C.-D. Gu, X.-L. Wang, An efficient route to a porous NiO/reduced graphene oxide hybrid film with highly improved electrochromic properties, Nanoscale 4 (2012) 5724-5730.

[70] I.Y. Cha, S.H. Park, J.W. Lim, S.J. Yoo, Y.-E. Song, The activation process through a bimodal transmittance state for improving electrochromic performance of nickel oxide thin film, Sol. Energy Mater. Sol. Cells 108 (2013) 22-26.

[71] S.V. Green, A. Kuzmin, J. Purans, C.G. Granqvist, G.A. Niklasson, Structure and composition of sputter-deposited nickel–tungsten oxide films, Thin Solid Films 519 (2011) 2062-2066.

[72] S.V. Green, E. Pehlivan, C.G. Granqvist, G.A. Niklasson, Electrochromism in sputter deposited nickel-containing tungsten oxide films, Sol. Energy Mater. Sol. Cells 99 (2012) 339-344.

[73] I. Valyukh, S.V. Green C.G. Granqvist, K. Gunnarsson, H. Arwin, G.A. Niklasson, Ellipsometrically determined optical properties of nickel-containing tungsten oxide thin films: Nanostructure inferred from effective medium theory, J. Appl. Phys. 112 (2012) 044308/044301–044308/044306.

[74] R.-T. Wen, G.A. Niklasson, C.G. Granqvist, Electrochromic iridium oxide films: Compatibility with propionic acid, potassium hydroxide, and lithium perchlorate in propylene carbonate, Sol. Energy Mater. Sol. Cells 120(2014) 151-156.

[75] R.-T. Wen, Electrochromism in Nickel Oxide and Iridium Oxide: Experimental Results, Licentiate Thesis, Uppsala University, Sweden, 2014.

[76] B.D. Cullity, S.R. Stock, Elements of X-ray Diffraction, third ed., Prentice-Hall, Upper Saddle River, NJ, USA, 2001.

[77] M. Mayer, SIMNRA, a simulation program for the analysis of NRA, RBS and ERDA, AIP Conf. Proc. 475 (1999) 541-544.

[78] J.A. Thornton, High-rate thick-film growth, Ann. Rev. Mater. Sci. 7 (1977) 239-260.

[79] C.G. Granqvist, Oxide-based electrochromic materials and devices prepared by magnetron sputtering, in D. Depla, S. Mahieu (eds.) Reactive Sputter Deposition in: D. Depla, S. Mahieu (eds.) Reactive Sputter Deposition, Springer, Berlin Heidelberg, Germany, 2008; pp. 485-495.

[80] E. Avendaño, A. Azens, G.A. Niklasson, C.G. Granqvist, Proton diffusion and electrochromism in hydrated NiO_y and $Ni_{1-x}V_xO_y$ thin films, J. Electrochem. Soc. 152 (2005) F203-F212.

[81] E. Avendaño, H. Rensmo, A. Azens, A. Sandell, G. de M. Azevedo, H. Siegbahn, G.A. Niklasson, C.G. Granqvist, Coloration mechanism in proton-intercalated electrochromic hydrated NiO_y and $Ni_{1-x}V_xO_y$ thin films, J. Electrochem. Soc. 156 (2009) P132-P138.

[82] H. Bode, K. Dehmelt, J. Witte, Zur Kenntnis der Nickelhydroxidelektrode – I. Über die Oxydationsprodukte von Nickel(II)-hydroxiden, Electrochim. Acta 11 (1966) 1079-1087.

[83] H. Bode, K. Dehmelt, J. Witte, Zur Kenntnis der Nickelhydroxidelektrode – II. Über das Nickel(II)-hydroxidhydrat, Z. Anorgan. Allgem. Chem. 366 (1969) 1-21.

[84] P. Chadwick, Continuum Mechanics: Concise Theory for Scientists and Engineers, Dover Publ., Mineola, NY, USA, 1999.

[85] S. Passerini, B. Scrosati, A. Gorenstein, The intercalation of lithium in nickel oxide and its electrochromic properties, J. Electrochem. Soc. 137 (1990) 3297-3300.

[86] S. Passerini, J. Scarminio, B. Scrosati, D. Zane, F. Decker, Thin metal oxide films on transparent substrates for Li-insertion devices, J. Appl. Electrochem. 23 (1993) 1187-1195.

[87] F. Decker, S. Passerini, R. Pileggi, B. Scrosati, The electrochromic process in non-stoichiometric nickel oxide thin film electrodes, Electrochim. Acta 37 (1993) 1033-1038.

[88] S. Passerini, B. Scrosati, Electrochromism of thin-film nickel oxide electrodes, Solid State Ionics 53–56 (1992) 520-524.

[89] T. Dutta, P. Gupta, A. Gupta, J. Narayan, Effect of Li doping in NiO thin films on its transparent and conducting properties and its application in heteroepitaxial p-n junctions, J. Appl. Phys. 108 (2010) 083715-7.